



Article

Advanced Progress Control of Infrastructure Construction Projects Using Terrestrial Laser Scanning Technology

Chengyi Zhang ¹ and David Arditi ^{2,*}

¹ Department of Civil & Architectural Engineering, University of Wyoming, Laramie, WY 82071, USA; chengyi.zhang@uwyo.edu

² Department of Civil, Architectural, Environmental Engineering, Illinois Institute of Technology, Chicago, IL 60616, USA

* Correspondence: arditiiit.edu; Tel.: +1-312-567-5751

Received: 11 September 2020; Accepted: 9 October 2020; Published: 12 October 2020



Abstract: Effective progress control is vital for steering infrastructure construction to completion with minimum delay. Walking through the infrastructure project site to record progress in different activities is time-consuming, requiring information extracted from construction drawings, schedules, and budgets, as well as data collected from the construction site. This process can be automated by using advanced remote sensing technologies. This study contributes to progress monitoring in large horizontal infrastructure projects. It presents a practical automated method using laser scanning technology that can track the project's progress in a real construction environment with limited human input. It is robust and accurate and is currently operational. The system capitalizes on the success of laboratory experiments. This system deals with occlusions effectively, accelerates the registration process of multiple scans, reduces the noise in the data, recognizes the objects of irregular shape, and is economically feasible. It provides evidence that all current challenges encountered in using laser scanners in monitoring construction progress can be overcome. This method has been successfully tested in the Wacker Drive reconstruction project in Chicago, IL.

Keywords: construction management; construction scheduling; progress control; laser scanning

1. Introduction

Effective monitoring of the progress of infrastructure construction is a key function of construction management as the information obtained is critical in evaluating periodic payment requests submitted by the contractor [1]. Construction managers record construction progress in different project stages and ensure that the project is on schedule. This is a time-consuming [2] and labor-intensive process [3,4]. It also presents safety concerns as infrastructure construction sites are complex, dynamic, and dangerous places. Indeed, the construction industry has the highest number of fatalities of any industry, accounting for over 18% of all fatal occupational injuries [5]. A more accurate, safer, and more robust method to monitor progress is needed for large scale construction projects, especially infrastructure projects.

Over the years, many researchers have made attempts to automate this process. For example, Abeid and Arditi [6] developed an automated real-time monitoring system that links time-lapse digital movies of construction activities, a critical path schedule, and visual progress control techniques. Golparvar-Fard et al. [7] proposed an image-based method using daily photographs taken from a construction site for progress control. They calibrated and reconstructed a series of images of the site to point cloud data. Then, they visually compared as-built data with 3D as-planned data and monitor the progress. Mejl ander-Larsen [8] developed a three-step process for reporting progress using building information modeling (BIM) to minimize manual reporting and increase quality and accuracy.

3D Laser scanning technology has been gaining increased recognition in construction management applications. Generally, 3D laser scanning technology is useful for owners, architects, designers, engineers, contractors, and inspectors to perform quality assurance and quality control [9], analyze deviations between as-built and as-designed structures [10,11], develop as-built drawings [12,13], monitor project progress [1,4,7,14–20], and assess damage caused by disasters [21].

Three-dimensional (3D) laser scanners have been investigated in the construction industry and have shown potential for supporting progress tracking [1,4,14,16,18,19]. Girardeau-Montaut et al. [22] worked on the applications of laser scanning technology to observe the changes at construction sites and inside facilities. Bosché et al. [23] developed a system fusing a 4D model and laser scanning for construction progress control purposes. Bosché et al. [10] and Bosché and Haas [24] obtained promising results of progress monitoring using a 3D laser scanner and a simple 3D model. Bosché et al. [23] introduced a quasi-automated approach for project progress tracking by fusing 3D CAD modeling and time stamped 3D laser scanned data. Based on his research, Turkan et al. [1] developed a system that is able to extract useful data for progress tracking. Cheok et al. [25,26] assessed and documented the construction process in real-time based on 3D as-built models by using laser scanning technology. Puri and Turkan [4] proposed a framework to utilize point cloud data obtained and 4D design models to identify deviations in the performed work from the planned work. Braun et al. [15] describe a concept for an automated comparison of the actual state of construction with the planned state for the early detection of deviations in the construction process. Arastounia [27] enhanced the algorithm of automatically recognizing rail racks and power cables using data obtained from terrestrial and airborne point clouds. Kumar et al. [28] developed an active contour model by extracting road edges from laser scanning data for roadway feature identification and management. Kim et al. [16] developed a three-phase method to align the as-built data with the as-planned model, to match the as-built data to the BIM, and then update the as-built status. Zhang and Arditi [20] developed an automated system that can assess progress control in laboratory conditions with minimum human input using laser scanning technology. Xu and Turkan [29] developed a new framework that implements camera-based unmanned aerial systems (UASs) with computer vision algorithms to collect and process inspection data, and Bridge Information Modeling (BrIM). Kim et al. [17] proposed a method for automated coarse registration of 3D point clouds with project 3D models that supported the proposed automated progress control method. Sadeghi et al. [30] developed an automated measurement system to calculate railway ballast geometry. Funari et al. [31] proposed a visual programming method to assess the historic masonry structures. Griebel et al. [32] reviewed the reliability and limitations of using terrestrial laser scanners to monitor forest canopy dynamics. Concerning geotechnical studies, Hashash et al. [33] successfully demonstrated calculating volumes of earthwork by using point cloud data, and Finno and Hashash [34] were able to monitor adjacent deformations and ground movements by using laser scanning technology. Abellán et al. [35] developed a procedure to detect and predict rockfalls using terrestrial laser scanning technology.

All the research studies mentioned above were conducted in the laboratory or involved relatively small-scale projects. In contrast, this paper is an attempt to monitor construction progress in real-life large infrastructure projects by making sure the barriers normally encountered in progress control are overcome, i.e., objects are easily identified using the objects' 3D coordinates, reliable point cloud data are captured despite occlusions, and the status of a project is compared at different times using the objects' shape definition and geometry information while allowing for tolerances. The objective of this study is to develop an advanced progress measurement method that automates these processes in monitoring progress in horizontal construction projects. It modifies the method developed by Zhang and Arditi [20] in laboratory conditions. This study first proposes a step by step workflow of automating construction progress control. Second, each step of the process is discussed in detail. Third, the proposed system is tested in a real-world infrastructure project. Finally, the results, benefit, significance and limitations of the study are discussed in detail. This system can reduce the time spent on this activity, reduce the safety risk, reduce the number of personnel used, reduce the cost

involved, reduce disagreements between contractor and owner, and add to the overall efficiency of project management. The Wacker Drive reconstruction project in Chicago is selected as a case study. The effects of weather, noisy data, and irregularly shaped objects are considered in the study as well as the cost and time implications of the method. This method has proved to be robust and accurate in the Wacker Drive reconstruction project, can be applied to any infrastructure construction project, and is currently operational.

2. Proposed System

This section describes the steps adopted in this study to identify the objects whose progress will be measured in a 3D model, to capture the point clouds after scanning the area, and to compare the information in the point cloud against the 3D model. The system is tested in a real-life construction project with objects of different shapes and occlusions. The progress recording/monitoring process is presented in Figure 1.

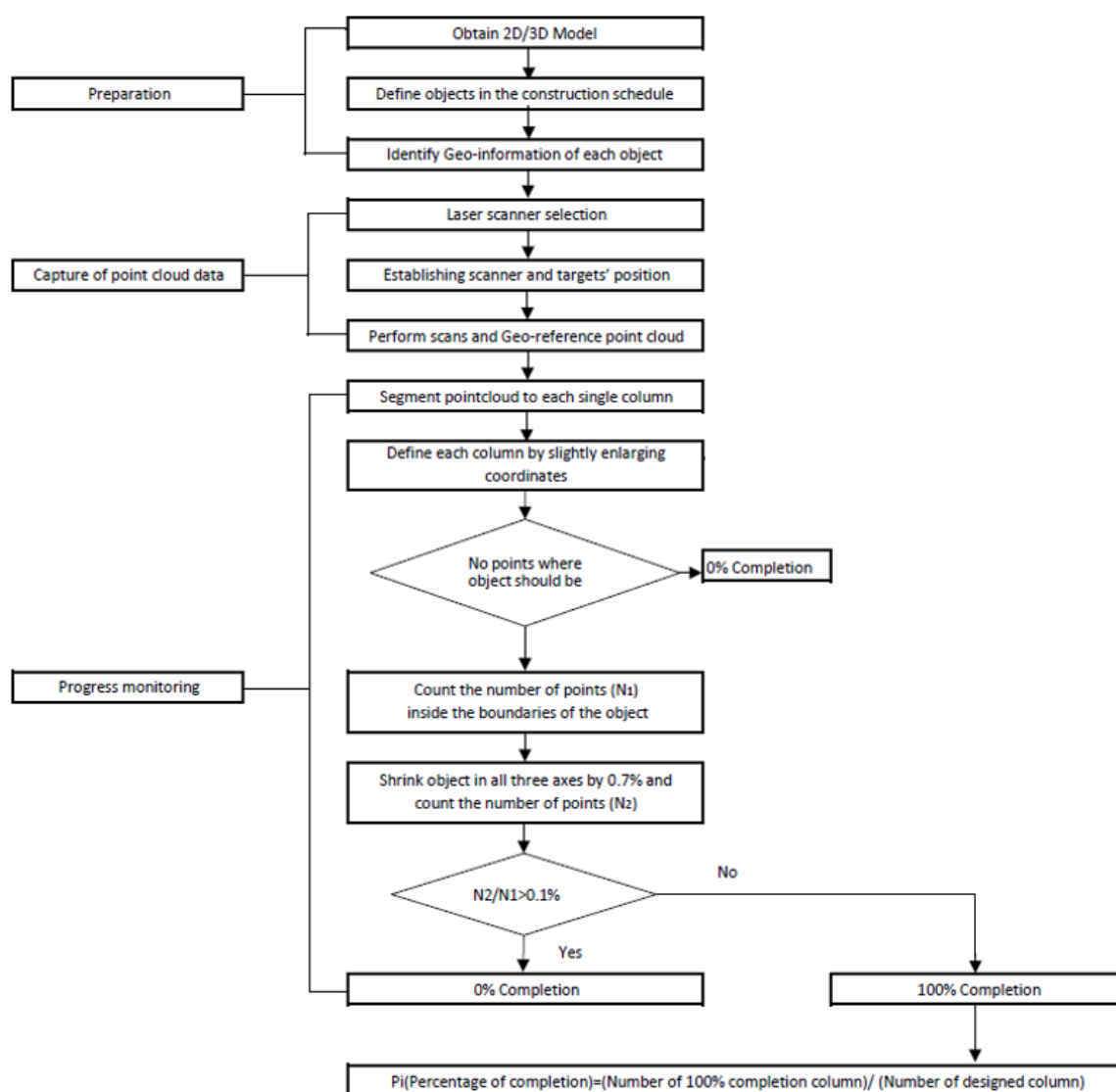


Figure 1. Progress recording and monitoring process.

2.1. Identification of Objects

A 3D model of the project is created. The activities of the project are defined based on the construction schedule. The objects involved in each activity are identified. From earlier survey

information, the objects' 3D coordinates are acquired, and equations are developed to calculate the volume/surface area of the objects involved in each activity.

2.2. Capture of Point Cloud Data

A laser scanner is selected by considering factors such as the range and accuracy specifications of the scanner, the accuracy requirements of the project, the cost of the scanner, as well as the budget of the entire project.

Time-of-flight scanners are commonly used for civil engineering projects. They emit a pulse of light, which measures the amount of time it takes to travel from the scanner to the object and back, allowing the scanner to calculate the distance. A single scan may last several minutes to a few hours, depending on the resolution setting and the scanner's mechanical system. The key benefit of this type of laser scanning technology is its long range. It is typically used for topographic surveys of roadways and as-built infrastructure [9,13,36,37]. Alba et al. [38] listed some time-of-flight scanners that can reach a range of more than 1 km to capture infrastructure systems, such as dams or bridges. The major limitation of time-of-flight scanning systems is their relatively low data collection rates. Even though the latest time-of-flight scanner on the market today can reach up to one million points per second, the majority of the scanners still have low collection rates compared to phased-base scanners.

Phase-based scanners use a different distance-measuring principle to achieve a much higher data collection rate relative to time-of-flight systems. Phase-based scanners are typically used in industrial applications or interior architectural spaces to populate detailed building information models of existing facilities. The advantage of this technology is the significant speed of data capture. It can capture hundreds of thousands to millions of 3D points per second, which is approximately ten times faster than most time-of-flight scanning systems [39]. The major limitation is the short range. The best working range for most phase-based scanners is less than 100 m. Beyond that range, noisy data will increase sharply due to range ambiguity issues, mixed pixels [39], and other technical problems. Those noisy data at object boundaries can cause inaccurate measurements of object dimensions and may mislead decisions about construction operations [39]. In all, phase-based laser scanners have a shorter maximum effective range than time-of-flight scanners, but have much higher data collection rates than time-of-flight scanners.

In this research, several measures were considered to optimize data collection. Before starting laser scanning, the environment of the project should be evaluated to determine the best time to collect data in order to minimize noisy data caused by human/equipment traffic or other factors. Further, obstructions should be identified that may cause data voids or shadows. Scanning in foggy, rainy, snowy, smoky, or poor weather conditions should be avoided.

The scanner set-up plays an important role in the quality of the resulting point cloud [40]. The ideal set-up is to position the laser scanner in such a way that the laser beam is near perpendicular to the surface of the object. Such an ideal set-up may not always be possible in practice. The different incidence angles and ranges of the laser beam on the object's surface may result in 3D points of varying quality [41]. The location of the scanner was carefully established before scanning was performed. The scanner was placed where no obstacles existed and on a stable footing. A bridge deck with much traffic may not be a good place to perform scanning. A tall tripod or high position was used to help reduce noise and avoid obstructions from traffic and pedestrians. The distance of the scans was determined by taking into consideration site conditions, project requirements, and the available scanners. Some areas that are difficult to scan were identified at the beginning. Multiple scans were performed to minimize the effects of occlusion. A better resolution setting or additional setups increase scan density and may help with accuracy.

In the original 3D design, each object has its location information. In order to define each object in the point clouds, the data should be in the same coordinate system. Targets are used to adjust, geo-reference, and combine different scans together in the registration step. A target can be stuck on

a surface (Figure 2a), a spherical target shown in Figure 2b can be mounted on a pole, or a tilt-and-turn planar target shown in Figure 2c can be installed.



(a) Sticky paper target. (b) Sphere target (c) Tilt and turn planar target

Figure 2. Different types of targets.

The setup of the targets is important as they directly influence the accuracy of the registration. This process is necessary to combine individual scans together. The targets should be placed evenly throughout the scan area, as shown in Figure 3. With at least one target in each quadrant, targets should be placed at different elevations and at the recommended optimal distance from the scanner according to the scanners’ manual.

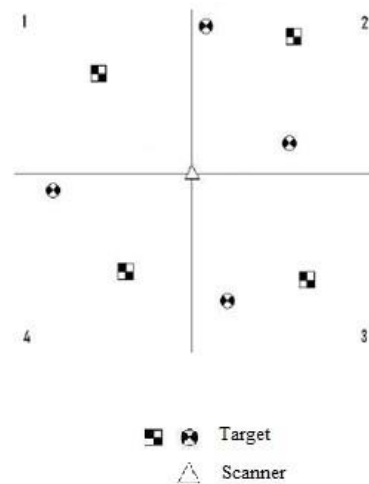
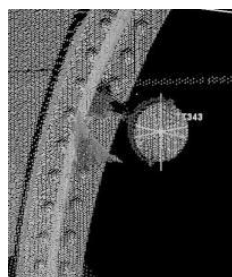
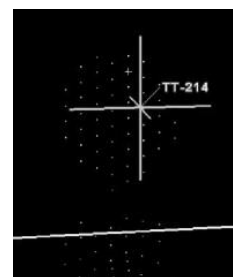


Figure 3. Example target layout.

Different laser scanning targets are designed for different distances. They should be scanned within the specified distance in order to get enough density to pinpoint their centers for registration purposes. A good target should have enough point cloud coverage, and the center of the target should be clearly shown, as in Figure 4a. If the distance from the scanner to the target exceeds the manufacturer’s recommended distance, it is hard to pinpoint the center of the target, as shown in Figure 4b, creating serious errors during registration.



(a) Within the recommended distance, with enough point cloud coverage.



(b) Beyond recommended distance, with very low point cloud density.

Figure 4. Effects of different distances between scanner and target.

Typically, for surveying applications, after scans are performed for modeling, surveying, and other purposes, the data obtained in the multiple scans should be manually registered to create a complete model space. However, in progress control, the only concern is the coordinates of the location of the points. Before a scan is performed, information about a coordinate system should be input into the scanner to record point cloud data relative to this system, hence eliminating the manual registration process. As a result, the process of progress control can be accelerated. Some scanners provide this function.

2.3. Progress Monitoring

In this research, the shapes of objects are not limited to prisms, as was the case in Zhang and Arditi’s (2013) original research. Two types of objects are considered. One is a cylindrical column, as shown in Figure 5a. Enlarging and shrinking cylindrical columns in all three dimensions can be achieved by changing the height (H) and radius (R), as shown in Figure 5b. The second type of object is a column used in expansion joints to connect two decks, as shown in Figure 5c. It is more complicated than the first type. To simplify the system and make it more efficient, only the bottom part is taken into consideration (Figure 5d). It is of course possible to monitor the completion of any object (e.g., beam, slab, wall units, etc.) over different time slices (e.g., weeks, months, etc.).

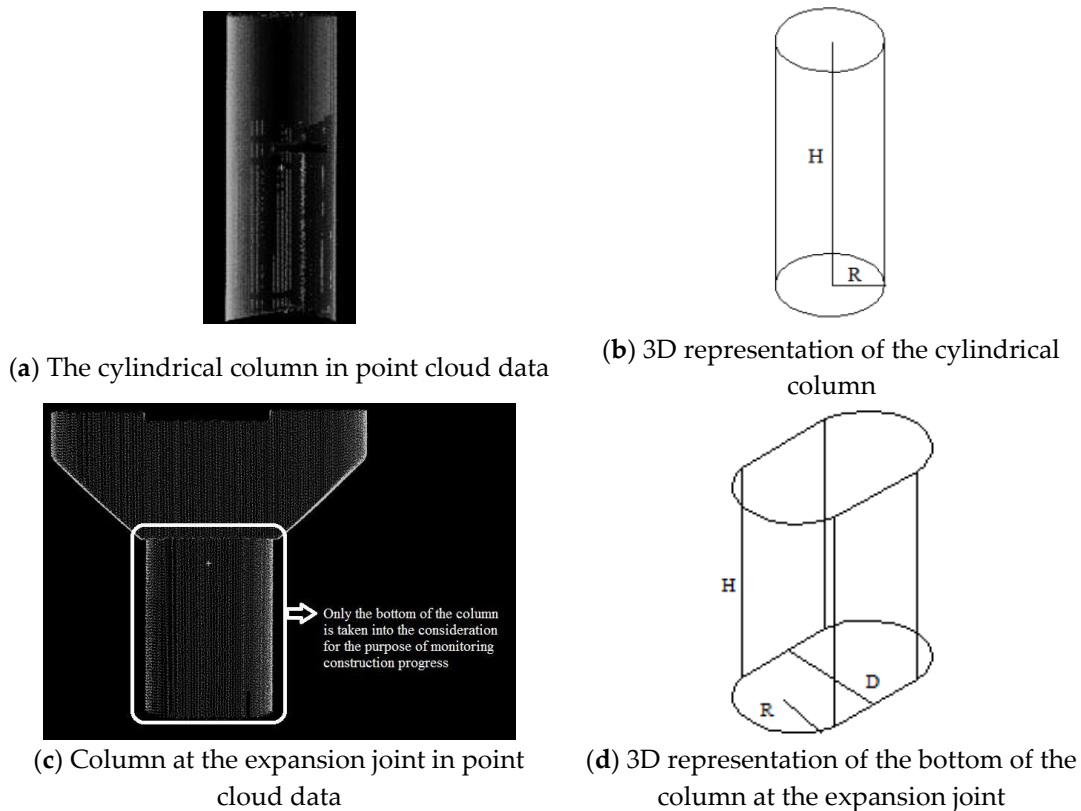


Figure 5. Types of columns used in the project.

From a construction progress perspective, the status of the column is either 0% or 100% complete since each column is poured in one batch. Once the bottom is completed, the column is considered to be 100% complete. Thus, counting the number of completed columns monitored progress. The column can be enlarged and shrunk in all three dimensions by changing the height (H), radius (R), and width (D), as shown in Figure 5d.

The 3D models of these two types of columns containing geo-location information are created in Microstation in the design phase. Each column has its own shape definition and geometry information

that are programmed to enlarge or shrink the object in the perpendicular direction to the object’s face. To account for construction and laser scanner tolerances, the true coordinates of the object in the 3D model are augmented by 0.7%, increasing the volume of the object by 2%, following El-Omari and Moselhi’s [42] observation in their laser scanner experiments. The points associated with the object need to be extracted from the original data. The number of points (N1) in the point cloud that falls within the augmented object is counted. If no points are found after 0.7% enlargement, for example, $N1 = 0$, then the percentage of completion of this column is 0%. If there are points found after 0.7% enlargement, for example, $N1 \neq 0$, then the system moves to the second step to record the number of points N2 after the object is shrunk by 1.5%.

The choice of shrinking the object by 1.5% in all directions is based on El-Omari and Moselhi’s [42] work, where they found that with a 0.015o resolution angle, the volume of the object they measured by using the point clouds was larger by 2% from the actual volume. A Leica Scanstation has a maximum range of 300 m with up to 4000 points per second. At a 50 m range, it can achieve a position accuracy of 6 mm. The resolution angle is equal to $\tan^{-1} = 6 \text{ mm}/50,000 \text{ mm} = 0.007^\circ$, which is less than 0.015o. As the resolution angle is less than 0.015o, the Leica Scanstation has better resolution and accuracy than in El-Omari and Moselhi’s [42] work. Thus, the object, if it exists, can be within 0.7% of the original boundaries making the volume of the object within $\pm 2\%$. In the proposed method, the object is shrunk by 1.5% in all directions to account for a 0.7% tolerance on either side of the surface plus an additional 0.1% to compensate for the small difference between the resolution angles ($0.7\% + 0.7\% + 0.1\% = 1.5\%$).

After the object is shrunk by 1.5%, if $N1/N2 \leq 0.1\%$, the column is considered to be 100% complete. If $N1/N2 > 0.1\%$, then it is concluded that the point clouds have nothing to do with the object, the percentage of completion of the column is 0%. The principle to determine if the point cloud data represent an object was developed in the study performed by Zhang and Arditi [20], and is shown in Figure 6 for a cylindrical column, and in Figure 7 for a column at an expansion joint.

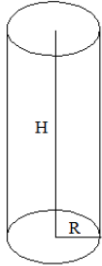
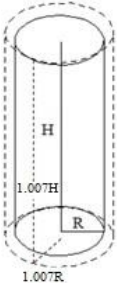
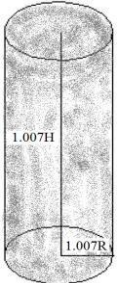
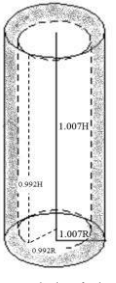
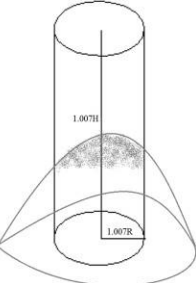
					
<p>3D Model of the column</p>	<p>3D Model of the column after it is enlarged by 0.7% in all three dimensions superimposed on point clouds. Number of points: N1</p>	<p>3D Model of the column after it is enlarged by 0.7% in all three dimensions superimposed on point clouds. Number of points: N1</p>	<p>3D Model of the column after it is shrunk by 1.5% in all three dimensions superimposed on point clouds. Number of points: N2</p>	<p>3D Model of the column after it is enlarged by 0.7% in all three dimensions superimposed on point clouds. Number of points: N1</p>	<p>3D Model of the column after it is shrunk by 1.5% in all three dimensions superimposed on point clouds. Number of points: N2</p>
<p>(a) $N1 = 0$. The object is not in place. (0% completion)</p>		<p>(b) $N2/N1 \leq 0.1\%$. Point cloud represents full object (100% completion)</p>		<p>(c) $N2/N1 \geq 0.1\%$. Point cloud represents another object (0% completion)</p>	

Figure 6. Interpretation of point clouds for the cylindrical column.

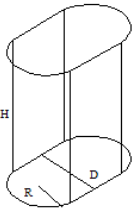
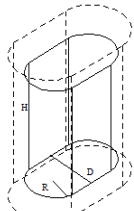
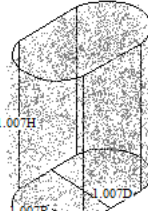
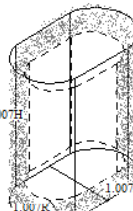
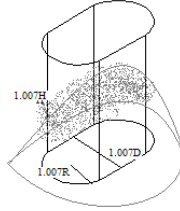
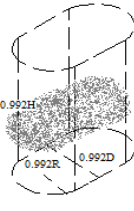
					
<p>3D model of the column</p>	<p>3D Model of the column after it is enlarged by 0.7% in all three dimensions superimposed on point clouds. Number of points: N_1</p>	<p>The column after it is enlarged by 0.7% in all three dimensions superimposed on point clouds. Number of points: N_1</p>	<p>3D Model of the column after it is shrunk by 1.5% in all three dimensions superimposed on point clouds. Number of points: N_2</p>	<p>The column after it is enlarged by 0.7% in all Three dimensions superimposed on point clouds. Number of points: N_1</p>	<p>3D Model of the column after it is shrunk by 1.5% in all three dimensions superimposed on point clouds. Number of points: N_2</p>
<p>(a) $N_1 = 0$. The object is not in place. (0% completion)</p>		<p>(b) $N_2/N_1 \leq 0.1\%$. Point cloud represents full object (100% completion)</p>		<p>(c) $N_2/N_1 \geq 0.1\%$. Point cloud represents another object (0% completion)</p>	

Figure 7. Interpretation of point clouds for a column at an expansion joint.

Two progress reports are generated. Progress is calculated by comparing the number of built columns and the number of planned columns in different scans, as shown in Equation (1).

$$P_{ij} = (n_1 + n_2 + n_3 + \dots + n_i)/N_j \tag{1}$$

where:

P_{ij} : Progress of completion in Section_{*j*} after Scan_{*i*} was performed n_i : Number of the constructed columns in Scan_{*i*} ($i = 1, 2, 3 \dots 23$) N_j : Number of the designed columns in Section_{*j*} ($j = 1, 2, 3 \dots 10$)

Progress in the total project is calculated by comparing the number of built columns and the number of planned columns in different scans, as shown in Equation (2).

$$P_i = (n_1 + n_2 + n_3 + \dots + n_i)/N_0 \tag{2}$$

where:

P_i : Percentage of completion after Scan_{*i*} was performed. n_i : Number of completed columns after Scan_{*i*} performed. N_0 : Number of the designed columns

3. Case Study

Wacker Drive is the cornerstone of architect Daniel Burnham’s 1909 vision for the rebuilding of Chicago. At the beginning of the new millennium, the original upper deck was crumbling, and the entire roadway did not meet modern standards for road widths and clearances. Restricted clearances, substandard merge lanes, and dangerous intersections contributed to the roadway’s problems. The Chicago Department of Transportation (CDOT) performed the reconstruction of historic Wacker Drive in 2001–2002. This project aimed to rebuild and restore east/west Wacker Drive (upper and lower), i.e., the oldest and most deteriorated segment of Wacker Drive located between Michigan Avenue and Randolph Street. It aimed to improve access and safety, ease traffic flow, and enhance the streetscape. The objectives also included improving access on lower Wacker Drive for deliveries to existing and expanding businesses and meet today’s design standards. For example, Lower Wacker

Drive had a substandard vertical clearance of 12.3 feet. The 20-month, \$200-million project was completed on time and within budget. Overall, the project contributed to creating a distinct look for Wacker Drive, as well as improving safety and operations of the roadway, creating a connection between the riverfront and the Loop, developing consistent intersections, and maximizing median areas for green space.

3.1. Identification of Objects

Column and deck designs were provided by the City of Chicago. Construction was conducted in sections under three separate contracts. This study considers Contract A that covers the portion of Wacker Drive between N. Franklin Street and N. State Street with a total length of 0.4 miles. This part of Wacker Drive runs alongside the Chicago River. It intersects with five streets, including Wells, LaSalle, Clark, Dearborn, and State Streets. The construction schedule was also provided by the Chicago Department of Transportation, as shown in Figure 8. Progress control involves monitoring and comparing the number of completed columns every day.

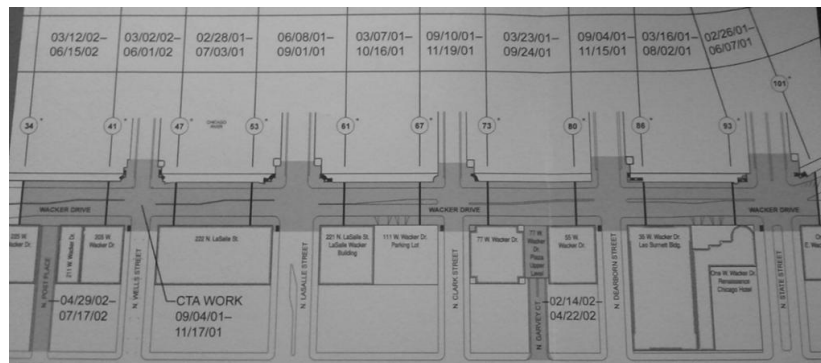


Figure 8. Construction schedule [43].

In total, there were 68 bents with 261 columns. Please note that, in some areas such as Section 6 (N. LaSalle Street), many columns belonged to the Chicago Riverwalk, which is an open pedestrian waterfront located on the south bank of the Chicago River. Those columns were excluded from this research. To simplify the schedule and make it easy to explain, a simple schedule was established, as shown in Figure 9. The construction order followed the section numbers. For example, Section 1 (N. State Street) was the first section constructed.

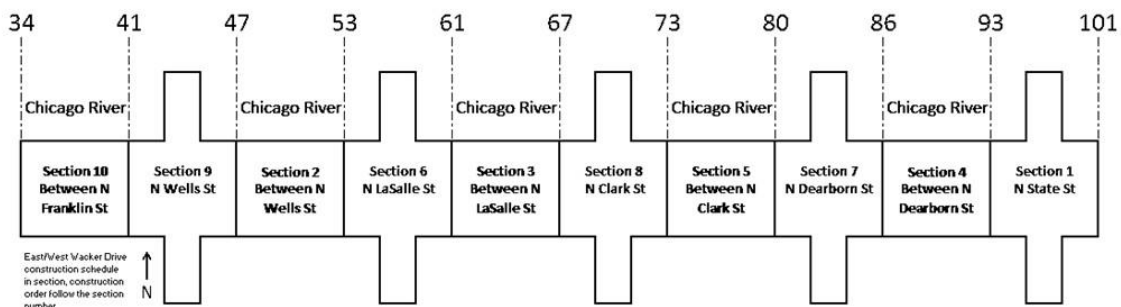


Figure 9. Construction Schedule for research.

From earlier preliminary survey information, each column was geo-referenced by using the project’s coordinate system. The geo-reference information of the columns in N. State Street is presented as an example in Figure 10. The labeling method used in the original design was also used in the research, starting from bent 34 to bent 101 in the west-east direction, row A to row D in the south-north direction.

Bent	Column	Northing	Easting	Street	Location
94	94A	902120.06	176276.36	N State St	
	94B	902152.45	176276.04		
	94C	902185.08	176275.71		
	94D	902217.55	176275.52		
95	95A	902120.25	176300.34	N State St	
	95B	902152.75	176300.01		
	95C	902185.29	176299.77		
	95D	902217.65	176299.55		
96	96A	902120.41	176326.29	N State St	
	96B	902152.99	176325.96		
	96C	902185.42	176325.52		
97	97A	902120.74	176352.22	N State St	
	97B	902153.24	176352.03		
	97C	902185.61	176351.75		
	97D	902218.17	176351.49		
98	98A	902120.89	176376.26	N State St	
	98B	902153.36	176375.95		
	98C	902185.88	176375.72		
	98D	902218.43	176375.52		
99	99A	902121.02	176406.43	N State St	
	99B	902153.59	176406.14		
	99C	902185.98	176405.86		
	99D	902218.56	176405.50		
100	100A	902121.41	176441.51	N State St	
	100B	902153.87	176441.26		
	100C	902186.35	176441.00		
	100D	902218.98	176440.77		
101	101A	902122.21	176475.02	N State St	
	101B	902154.17	176474.72		
	101C	902186.65	176474.45		
	101D	902219.07	176474.26		

Figure 10. Column Geo-referenced locations in N. State St.

The 3D model of the lower Wacker Drive was created in MicroStation based on the 2D design in DGN format. Each column was assigned a position in its own layer with location information. The geo-information of the 3D model was extracted to calculate the number of points in the point clouds of the objects involved in each activity. Figure 11 presents an example of a 3D model of the columns and deck in N. State Street.

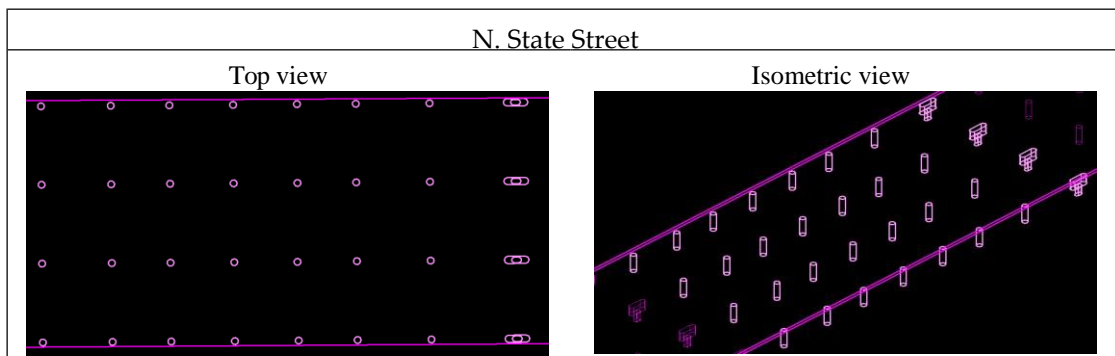


Figure 11. 3D Model of Columns and decks.

3.2. Capture of Point Cloud Data

The original intent of the scans was to perform topographic surveys of the Wacker Drive reconstruction project. Time-of-flight technology is typically used for this purpose because a long-range scanner minimizes setup and scanning times. Therefore, the Leica Scanstation (a time-of-flight scanner) was used to capture point cloud data. Progress control was a by-product of this activity. For monitoring construction progress, the density of point clouds does not need to be very high; cost and time are more important than point density.

In the preparation phase, the survey team used a total station to capture the coordinates of pre-georeferenced targets. Before performing scanning, the scanner was tied down to the Wacker drive coordinate system.

In this project, the longest span among each section is 225 feet, and the shortest span is 175 feet. The average distance between two adjacent columns is 28 feet. Based on the preliminary construction schedule, three or four scans were scheduled for each section, and each scan was designed to have maximum coverage of three bents with a total of 12 columns. The scanner was typically set up in the location shown in Figure 12 to have full coverage of the objects' surface and to avoid occlusions.

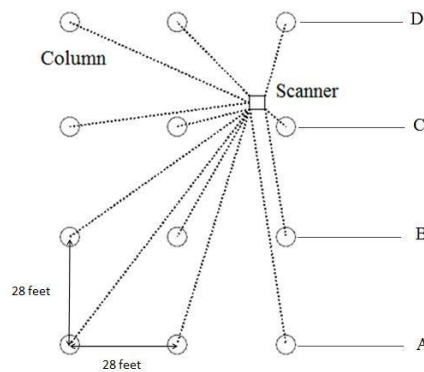


Figure 12. Location of the scanner in a typical section.

Due to the conditions in the construction site, an ideal setup was not possible. The location of the scanner depended on the situation in the field. In addition, scans were performed before or after work hours, typically in the early morning or late evening to avoid people and traffic. The layout of the scanner's locations is shown in Figure 13. In total, 23 scans were performed in this study.

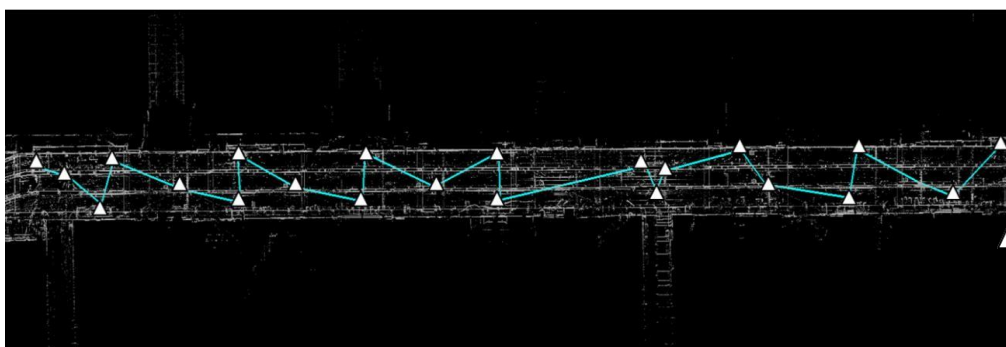


Figure 13. Scanner locations.

The Lower Wacker Reconstruction project used its own coordinate system rather than World Geodetic System 84 (WGS84) or the State plane coordinate system. Fifty-five control points were set up and input into the scanner before it started scanning. The original point cloud data came with the correct coordinate information, and therefore no registration process was needed.

3.3. Progress Monitoring

As seen in Figure 9, the ten sections are similar to each other, and only Section 1 (N. State Street) is selected to describe the process. N. State Street has 8 bents, from bent 94 to bent 101, with 32 columns in total. In order to catch the progress, scans were performed on three different days. Each day, three scans were performed in the same location. The location of each scan is shown in Figure 14.

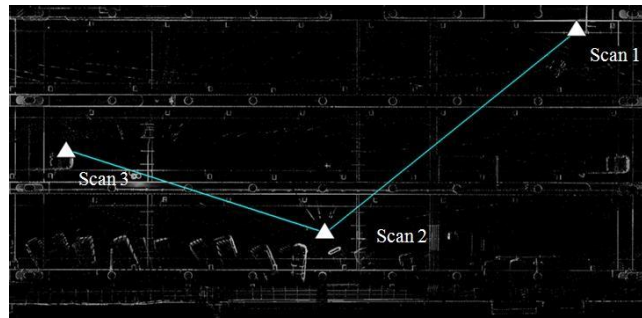
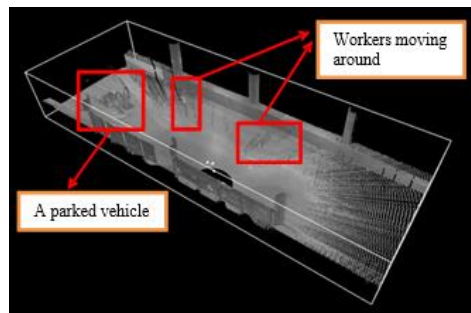
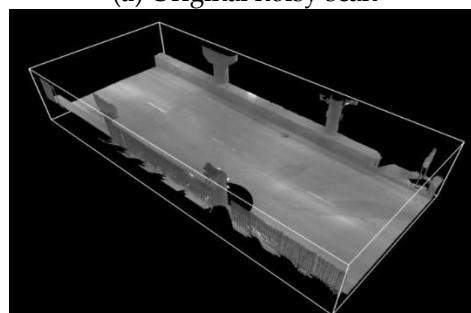


Figure 14. Scanner’s location in Section 1 (N. State St.).

The scans were named Scan1, Scan 2, and Scan 3. Each scan was set up to have full coverage of the columns. There was no large construction equipment such as trucks and shovels on the construction site during the scanning of the area because scans were performed in the late evening or early morning. Only a portion of a small vehicle and few workers were captured by the scanner. As columns were typically 10 ft high, there was no full occlusion of any column. Two operations had to be performed to measure progress. First, due to the conditions on the site, the range of the laser beam was limited to only 100 ft (30 m), although the scanner can reach up to 1000 ft (300 m). The reason for choosing 100 ft (30 m) was because the scanner was located such that it had enough coverage of no more than three bents, i.e., up to 100 ft (30 m). By limiting the range of the laser beam to 100 ft (30 m), it was possible to eliminate useless data in the scans, hence avoiding handling a very large amount of point cloud data. Second, the “region grow” technique was used to reduce the noise in the data and smooth out the information about the pavement. Figure 15a shows the original scan with the noisy data caused by workers moving around and a parked vehicle. In Figure 15b, the region grow parameters were defined to control the thickness of the pavement, the level of detail, and the size of the region. Figure 15c shows the results of the “region grow” process with a clear view of the pavement.

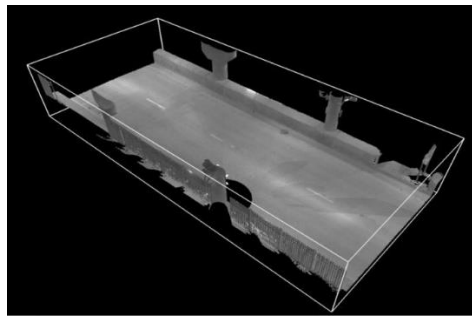


(a) Original noisy scan



(b) Performing region grow

Figure 15. Cont.



(c) Clean area

Figure 15. Region grow process.

Take Column 94A as an example. The number of points recorded after enlarging Column 94A 0.7% in all three dimensions is $N_{94A1} = 12,293$. Then, shrinking the column’s dimensions by 1.5% in all three dimensions, no points were observed ($N_{94A2} = 0$), which indicates that Column 94A is 100% complete since the ratio $N_{94A2}/N_{94A1} = 0$ is less than 0.1%. This process was applied to every column. Progress reports were issued after the last iteration was performed ($N_{scan1} = 12$ columns).

After Scan 1 was performed, progress was calculated as follows:

$$P_{11} = (n_1 + n_2 + n_3)/N_1 = 12/32 = 37.5\%$$

where:

P_{11} = Percentage of columns completed in Section 1 (Scan 1)

n_1 = 12 columns completed in Section 1 (Scan 1),

n_2, n_3 = Scans 2 and 3 not performed

N_1 = 32 columns planned in Section 1

$$P_1 = (n_1 + n_2 + n_3 + \dots + n_{23})/261 = 12/261 = 4.6\%$$

where:

P_1 = Percentage of columns completed (Scan 1)

n_1 = 12 columns completed in Section 1 (Scan 1)

$n_2 \dots n_{23}$ = Scans 2 to 23 not performed

N_1 = Total 261 columns planned in Section 1 to Section 10

After Scan 2 was performed, progress was calculated as follows:

$$P_{21} = (n_1 + n_2 + n_3)/N_1 = (12 + 12)/32 = 75\%$$

$$P_2 = (n_1 + n_2 + n_3 + \dots + n_{23})/261 = (12 + 12)/261 = 9.2\%$$

After Scan 3 was performed, progress was calculated as follows:

$$P_{31} = (n_1 + n_2 + n_3)/N_1 = (12 + 12 + 8)/32 = 100\%$$

$$P_3 = (n_1 + n_2 + n_3 + \dots + n_{23})/261 = (12 + 12 + 8)/261 = 12.2\%$$

There were a total of 32 columns in Section 1, and after three scans were performed, the system detected 32 columns that were in place; progress in Section 1 was $32/32 = 100\%$, and progress in the entire project was 12.2%, as shown in Figure 16. As can be seen in Figure 16, the number of points before shrinking (N_1) and the number of points after shrinking (N_2) are recorded for each column as

well as the ratio N_2/N_1 . If the column is defined as a constructed column by the program, then Y (Yes) is marked in the last column. If not, then N (N_0) is marked. This process was applied to all ten sections for all 261 columns.

Scan	Bents	Column	Street Name	Number of point before shrinking (N_1)	Number of point after shrinking (N_2)	N_2/N_1	Finish	Percentage of completion in Section (P_i sectionj)	Percentage of completion in total (P_i)
Scan 1	94	94A	N State St	12293	0	0	Y	12/32=37.5%	12/261=4.6%
		94B		231191	0	0	Y		
		94C		36086	0	0	Y		
		94D		9013	0	0	Y		
	95	95A	N State St	18723	0	0	Y		
		95B		80248	0	0	Y		
		95C		32499	0	0	Y		
		95D		8906	0	0	Y		
	96	96A	N State St	28739	0	0	Y		
		96B		40091	0	0	Y		
		96C		21478	0	0	Y		
		96D		3646	0	0	Y		
Scan 2	97	N State St	97A	116461	0	0	Y	24/32=75%	24/261=9.2%
			97B	107459	0	0	Y		
			97C	8870	0	0	Y		
			97D	3976	0	0	Y		
	98	N State St	98A	32636	0	0	Y		
			98B	31237	0	0	Y		
			98C	16546	0	0	Y		
			98D	3715	0	0	Y		
	99	N State St	99A	10859	0	0	Y		
			99B	12305	0	0	Y		
			99C	18140	0	0	Y		
			99D	13308	0	0	Y		
Scan 3	100	N State St	100A	6329	0	0	Y	32/32=100%	32/261=12.2%
			100B	10964	0	0	Y		
			100C	36004	0	0	Y		
			100D	139882	0	0	Y		
	101	N State St	101A	7833	0	0	Y		
			101B	17934	0	0	Y		
			101C	56975	0	0	Y		
			101D	115475	0	0	Y		

Figure 16. Progress control in Section 1 (N. State St.).

This section may be divided by subheadings. It should provide a concise and precise description of the experimental results, their interpretation as well as the experimental conclusions that can be drawn.

4. Conclusions

This study successfully monitored progress in a real-life construction project. The Wacker Drive Reconstruction project in Chicago was selected as a case study. In this 0.4-mile reconstruction project, 23 scans were performed to generate a detailed record of the construction, to measure bridge clearance, and to monitor construction progress. All 261 columns were detected by the system. After each scan was performed, progress reports were created for each section and the entire project. The highlights of this study include issues related to occlusions, shapes of the objects to be monitored, the registration process, economic feasibility, and future improvements. The study’s contribution to laser scanning research and practice includes overcoming all current barriers encountered when laser scanners are used for monitoring construction progress. The study provides evidence that occlusions can be managed, objects with different shapes can be modeled, registration can be simplified, and the cost can be kept to a minimum. What is more, all this can be done in an automated way with minimum user interaction. The automation of this process is likely to reduce the duration of the inspection process and the laborious work of monitoring construction progress. It is also likely to enhance the personal safety of construction managers and inspectors. In the long term, it is expected that it will generate significant economic benefits since in the proposed method, progress-related data are collected as a by-product of the scanning process that is conducted as a routine project documentation activity rather than by an inspector that is specifically assigned to pursue progress control. The study showed that the results can be generalized for large horizontal infrastructure projects, especially for roadway, bridge, and railroad construction.

4.1. Occlusions

This study was conducted in a real-life construction project rather than in the laboratory. Occlusions that may occur in a real-life construction site were avoided by taking the following measures. First, the locations of the scanners were optimized to have enough coverage of each column. Second, the range of the laser beam was kept to only 100 ft (30 m) to eliminate useless data out of range, hence allowing the system to run more smoothly as it handles a smaller amount of point cloud data. Third, scans were performed in good weather. For example, construction in Section 1, N. State St. was started in February, which may bring cold, snow, and fog in the Chicago area. In order to ensure the accuracy of the point cloud data, scans were performed in good weather with clear sight. Fourth, scans were performed during the weekend, in the early morning or late evening. Many workers and construction equipment were on the construction site during daylight hours, which may block the view of the scanner and cause occlusions. Moving vehicles and people add noise to the point cloud data. Scans were performed in off-hours to avoid trucks, people, and piles of unrelated construction materials. Fifth, the region grow technology was used to automatically clean the small amount of noise left in the data caused by inevitable obstructions such as trucks, people, and construction materials. Sixth, even if parts of a column were blocked by obstructions, it was still possible to determine if the column was completed or not because a column cannot be half-completed, and because the columns were tall enough to be captured by the scanner despite possible occlusions. These measures allowed the system to run efficiently in calculating progress.

4.2. Shapes of Objects

The shapes of objects were not limited to prisms. Two types of columns were defined in this study, namely cylindrical columns, and columns at expansion joints. The 3D models of these two types of columns containing geo-location information were created in Microstation in the design phase. Each column had its shape definition and geometry information that was programmed to enlarge or shrink the object in the perpendicular direction to the object's face. This method can be applied to regular construction activities such as prismatic columns, cylindrical columns, masonry columns, concrete decks, pavement surfaces, pipes, and so on.

4.3. The Registration Process

Some instruments require that a registration process be performed manually to combine and geo-reference point cloud data. In this study, a Leica Scanstation was used to capture the point cloud data. This type of scanner allows the input of a coordinate system into the scanner before scanning starts. This process allows the point cloud data to be registered automatically within the scanner and be in the correct coordinate system. For modeling, surveying, and other applications, it might still be necessary to perform the manual registration process to have a full model space. However, for the purpose of monitoring construction progress, scans were treated individually in the correct location and did not need to be registered.

4.4. Economic Feasibility

The economic feasibility of the system was discussed in the context of other laser scanning applications. 3D laser scanning is a relatively new technology, and the cost of purchasing and deploying one or several laser scanners is not trivial. If one compares the traditional progress control method and the method of applying laser scanning in monitoring construction progress, it may be cheaper to send out a crew to inspect and record the percentages of completion in various activities rather than performing laser scanning. However, laser scanning technology brings many benefits to the construction manager, automating construction progress control being only a minor one. Laser scanning can be used for multiple purposes, including measuring distances and clearances, communicating between stakeholders, referring to recorded data for operation, maintenance, and

renovation/rehabilitation, and automating construction progress control. Progress monitoring with laser scanning can be economically feasible when used alongside other applications such as generating a detailed record of the construction or measuring clearances.

4.5. Limitation and Future Research

In the model presented in this research, geometry information about objects of different shapes is needed to shrink/enlarge the objects. A library of objects of different shapes could reduce the time and effort spent by the user. In addition, besides the terrestrial laser scanner, there is a variety of tools that can be used to collect point cloud data. Mobile laser scanning could be a good selection that can improve the capture of point cloud data. However, mobile scanners are not as accurate as terrestrial scanners, but high accuracy is not a must for progress control. Using mobile laser scanning technology in progress monitoring could be explored in the future. Additionally, the research established a solid foundation for automated progress control, but the full potential of digital modelling and analysis can be expanded in the future by exploiting the capabilities of laser scanning technology in creating digital twins in infrastructure performance.

Author Contributions: Conceptualization, D.A. and C.Z.; methodology, D.A. and C.Z.; case study, C.Z.; writing—original draft preparation, C.Z.; writing—review and editing D.A. and C.Z.; supervision, D.A. All authors have read and agreed to the published version of the manuscript.

Funding: This research received no external funding.

Conflicts of Interest: The authors declare no conflict of interest.

References

1. Turkan, Y.; Bosche, F.; Haas, C.T.; Haas, R. Automated progress tracking using 4D schedule and 3D sensing technologies. *Autom. Constr.* **2012**, *22*, 414–421. [[CrossRef](#)]
2. Navon, R.; Sacks, R. Assessing research issues in Automated Project Performance Control (APPC). *Autom. Constr.* **2007**, *16*, 474–484. [[CrossRef](#)]
3. Flanagan, R.; Marsh, L. Measuring the costs and benefits of information technology in construction. *Eng. Constr. Archit. Manag.* **2000**, *7*, 423–435. [[CrossRef](#)]
4. Puri, N.; Turkan, Y. Bridge construction progress monitoring using lidar and 4D design models. *Autom. Constr.* **2020**, *109*, 102961. [[CrossRef](#)]
5. Bureau of Labor Statistics. *US Department of Labor, Occupational Outlook Handbook, 2016–2017 ed.*; Bureau of Labor Statistics: Washington DC, USA, 2016.
6. Abeid, J.; Allouche, E.; Arditi, D.; Hayman, M. PHOTO-NET II: A computer-based monitoring system applied to project management. *Autom. Constr.* **2003**, *12*, 603–616. [[CrossRef](#)]
7. Golparvar-Fard, M.; Bohn, J.; Teizer, J.; Savarese, S.; Peña-Mora, F. Evaluation of image-based modeling and laser scanning accuracy for emerging automated performance monitoring techniques. *Autom. Constr.* **2011**, *20*, 1143–1155. [[CrossRef](#)]
8. Mejl ander-Larsen, Ø. A three-step process for reporting progress in detail engineering using BIM, based on experiences from oil and gas projects. *Eng. Constr. Archit. Manag.* **2019**, *26*, 648–667. [[CrossRef](#)]
9. Akinci, B.; Boukamp, F.; Gordon, C.; Huber, D.; Lyons, C.; Park, K. A formalism for utilization of sensor systems and integrated project models for active construction quality control. *Autom. Constr.* **2006**, *15*, 124–138. [[CrossRef](#)]
10. Bosch e, F.; Haas, C.; Murray, P. Performance of Automated Project Progress Tracking with 3D Data Fusion. In Proceedings of the CSCE 2008 Annual Conference, Quebec, QC, Canada, 10 June 2008.
11. Tang, P.; Huber, D.; Akinci, B.; Lipman, R.; Lytle, A. Automatic reconstruction of as-built building information models from laser-scanned point clouds: A review of related techniques. *Autom. Constr.* **2010**, *19*, 829–843. [[CrossRef](#)]
12. Arayici, Y. An approach for real world data modelling with the 3D terrestrial laser scanner for built environment. *Autom. Constr.* **2007**, *16*, 816–829. [[CrossRef](#)]

13. Jaselskis, E.J.; Gao, Z.; Walters, R.C. Improving Transportation Projects Using Laser Scanning. *J. Constr. Eng. Manag.* **2005**, *131*, 377–384. [[CrossRef](#)]
14. Braun, A.; Tuttas, S.; Borrmann, A.; Stilla, U. Automated progress monitoring based on photogrammetric point clouds and precedence relationship graphs. *Isarc. Proc. Int. Symp. Autom. Robot. Constr.* **2015**, *32*, 1.
15. Braun, A.; Tuttas, S.; Borrmann, A.; Stilla, U. A concept for automated construction progress monitoring using BIM-based geometric constraints and photogrammetric point clouds. *J. Inf. Technol. Constr.* **2015**, *20*, 68–79.
16. Kim, C.; Son, H.; Kim, C. Automated construction progress measurement using a 4D building information model and 3D data. *Autom. Constr.* **2013**, *31*, 75–82. [[CrossRef](#)]
17. Kim, C.; Son, H.; Kim, C. Fully automated registration of 3D data to a 3D CAD model for project progress monitoring. *Autom. Constr.* **2013**, *35*, 587–594. [[CrossRef](#)]
18. Pučko, Z.; Šuman, N.; Rebolj, D. Automated continuous construction progress monitoring using multiple workplace real time 3D scans. *Adv. Eng. Inform.* **2018**, *38*, 27–40. [[CrossRef](#)]
19. Teizer, J.; Lao, D.; Sofer, M. Rapid Automated Monitoring of Construction Site Activities Using Ultra-Wideband. In Proceedings of the 24th International Symposium on Automation and Robotics in Construction, Kochi, India, 19–21 September 2007. [[CrossRef](#)]
20. Zhang, C.; Ardit, D. Automated progress control using laser scanning technology. *Autom. Constr.* **2013**, *36*, 108–116. [[CrossRef](#)]
21. Olsen, M.J.; Kuester, F.; Chang, B.J.; Hutchinson, T.C. Terrestrial Laser Scanning-Based Structural Damage Assessment. *J. Comput. Civ. Eng.* **2010**, *24*, 264–272. [[CrossRef](#)]
22. Girardeau-Montaut, D.; Roux, M.; Marc, R.; Thibault, G. Change detection on point cloud data acquired with a ground laser scanner. *Int. Arch. Photogramm. Remote Sens. Spat. Inf. Sci.* **2005**, *36*, W19.
23. Bosché, F.; Turkan, Y.; Haas, C.; Haas, R. Fusing 4D Modelling and Laser Scanning for Construction Schedule Control. In Proceedings of the 26th Annual ARCOM Conference, Leeds, UK, 6–8 September 2010.
24. Bosche, F.; Haas, C.T. Automated retrieval of 3D CAD model objects in construction range images. *Autom. Constr.* **2008**, *17*, 499–512. [[CrossRef](#)]
25. Cheok, G.; Stone, W.; Lipman, R.; Witzgall, C.; Bernal, J. Laser Scanning for Construction Metrology. In Proceedings of the American Nuclear Society 9th International Topical Meeting on Robotics and Remote Systems, Seattle, WA, USA, 4–8 March 2001; pp. 1–10.
26. Cheok, G.S.; Stone, W.C.; Lipman, R.R.; Witzgall, C. Ladars for construction assessment and update. *Autom. Constr.* **2000**, *9*, 463–477. [[CrossRef](#)]
27. Arastounia, M. An enhanced algorithm for concurrent recognition of rail tracks and power cables from terrestrial and airborne lidar point clouds. *Infrastructures* **2017**, *2*, 8. [[CrossRef](#)]
28. Kumar, P.; Lewis, P.; McCarthy, T. The potential of active contour models in extracting road edges from mobile laser scanning data. *Infrastructures* **2017**, *2*, 9. [[CrossRef](#)]
29. Xu, Y.; Turkan, Y. BrIM and UAS for bridge inspections and management. *Eng. Constr. Archit. Manag.* **2019**, *27*, 785–807. [[CrossRef](#)]
30. Sadeghi, J.; Motieyan Najar, M.E.; Zakeri, J.A.; Kuttelwascher, C. Development of railway ballast geometry index using automated measurement system. *Meas. J. Int. Meas. Confed.* **2019**, *138*, 132–142. [[CrossRef](#)]
31. Funari, M.F.; Spadea, S.; Lonetti, P.; Fabbrocino, F.; Luciano, R. Visual programming for structural assessment of out-of-plane mechanisms in historic masonry structures. *J. Build. Eng.* **2020**, *31*, 101425. [[CrossRef](#)]
32. Griebel, A.; Bennett, L.T.; Culvenor, D.S.; Newnham, G.J.; Arndt, S.K. Reliability and limitations of a novel terrestrial laser scanner for daily monitoring of forest canopy dynamics. *Remote Sens. Environ.* **2015**, *166*, 205–213. [[CrossRef](#)]
33. Hashash, Y.M.A.; Marulanda, C.; Ghaboussi, J.; Jung, S. Novel approach to integration of numerical modeling and field observations for deep excavations. *J. Geotech. Geoenvironmental Eng.* **2006**, *132*, 1019–1031. [[CrossRef](#)]
34. Hashash, Y.; Asce, M.; Finno, R. Development of New Integrated Tools for Predicting, Monitoring, and Controlling Ground Movements due to Excavations. *Pract. Period. Struct. Des. Constr.* **2008**, *13*, 4–10. [[CrossRef](#)]
35. Abellán, A.; Calvet, J.; Vilaplana, J.M.; Blanchard, J. Detection and spatial prediction of rockfalls by means of terrestrial laser scanner monitoring. *Geomorphology* **2010**, *119*, 162–171. [[CrossRef](#)]

36. Soilán, M.; Sánchez-Rodríguez, A.; del Río-Barral, P.; Perez-Collazo, C.; Arias, P.; Riveiro, B. Review of Laser Scanning Technologies and Their Applications for Road and Railway Infrastructure Monitoring. *Infrastructures* **2019**, *4*, 58. [[CrossRef](#)]
37. Tang, P.; Akinci, B. Formalization of workflows for extracting bridge surveying goals from laser-scanned data. *Autom. Constr.* **2012**, *22*, 306–319. [[CrossRef](#)]
38. Alba, M.; Fregonese, L.; Prandi, F.; Scaioni, M.; Valgoi, P. Structural monitoring of a large dam by terrestrial laser scanning. *Int. Arch. Photogramm. Remote Sens. Spat. Inf. Sci.* **2006**, *36*, 6.
39. Tang, P.; Akinci, B.; Huber, D. Quantification of edge loss of laser scanned data at spatial discontinuities. *Autom. Constr.* **2009**, *18*, 1070–1083. [[CrossRef](#)]
40. Abu Hanipah, A.F.F.; Tahar, K.N. Development of the 3D dome model based on a terrestrial laser scanner. *Int. J. Build. Pathol. Adapt.* **2018**, *36*, 122–136. [[CrossRef](#)]
41. Lindenbergh, R.C.; Soudarissanane, S.S.; De Vries, S.; Gorte, B.G.H.; De Schipper, M.A. Aeolian Beach Sand Transport Monitored by Terrestrial Laser Scanning. *Photogramm. Rec.* **2011**, *26*, 384–399. [[CrossRef](#)]
42. El-Omari, S.; Moselhi, O. Integrating 3D laser scanning and photogrammetry for progress measurement of construction work. *Autom. Constr.* **2008**, *18*, 1–9. [[CrossRef](#)]
43. Wacker Drive Construction Project, Chicago, Ill. Department of Transportation, Bureau of Bridges and Transit, 2002. Available online: <https://www.worldtransitresearch.info/research/1555/> (accessed on 21 March 2020).



© 2020 by the authors. Licensee MDPI, Basel, Switzerland. This article is an open access article distributed under the terms and conditions of the Creative Commons Attribution (CC BY) license (<http://creativecommons.org/licenses/by/4.0/>).